TELKOMNIKA Telecommunication Computing Electronics and Control
Vol. 24, No. 1, February 2026, pp. 206~218
ISSN: 1693-6930, DOI: 10.12928/TELKOMNIKA.v24i1.27401

Distorted born iterative method reconstruction in high-noise environments using KNN-based machine learning denoising

Nguyen Quang Huy, Nguyen Truong Thang
Institute of Information Technology, Vietnam Academy of Science and Technology, Hanoi, Vietnam

Article Info

Article history:

Received Jul 15 2025
Revised Oct 23, 2025
Accepted Dec 8, 2025

Keywords:

Distorted born iterative method ultrasound
Inverse scattering
K-nearest neighbors
Tikhonov regularization
Tomography

ABSTRACT

Ultrasound tomography reconstruction using the distorted born iterative method (DBIM) is sensitive to measurement noise, which degrades image fidelity and slows convergence. We propose integrating a k-nearest neighbors (KNN) denoising step within each DBIM iteration to suppress noise adaptively while preserving structural edges. Simulations with a circular cylindrical target and transmit/receive geometry (12×12) were conducted at signal-to-noise ratio (SNR) levels of 6 dB, 3 dB, and 1 dB. Compared with conventional DBIM employing Tikhonov regularization, the KNN-filtered DBIM reduces normalized reconstruction error by up to 57.2% at 1 dB and shows faster error decay over successive iterations. The method is training-free, computationally lightweight, and preserves fine structural details. These properties make KNN-filtered DBIM attractive for noisy or resource-constrained imaging environments. Future work will validate the approach on experimental data and explore adaptive K selection.

Corresponding Author:

Nguyen Quang Huy
Institute of Information Technology, Vietnam Academy of Science and Technology
18 Hoang Quoc Viet, Cau Giay District, Hanoi, Vietnam
Email: quanghuy7889@gmail.com

1. INTRODUCTION

Ultrasound imaging and tomography are critical techniques in clinical diagnostics, providing non-invasive and real-time visualization of internal tissues. Traditional ultrasound image acquisition primarily relies on the pulse-echo method, where reflected signals from tissue boundaries are used to reconstruct the underlying structure of the imaged object [1]. However, this approach has inherent limitations in resolution and contrast, particularly in highly scattering media. To address these challenges, inverse scattering techniques have been developed, allowing for more accurate image reconstruction by incorporating multiple viewing angles around the object [2]. These methods enable improved imaging quality, especially under strong scattering conditions, making them suitable for biomedical applications such as breast cancer detection and soft tissue characterization. In ultrasound tomography, two primary imaging modalities are commonly studied: attenuation imaging and sound-speed imaging [3]. While attenuation images provide valuable information about tissue properties, sound-speed imaging generally offers superior resolution and contrast, making it a preferred choice for high-fidelity tomographic reconstructions. Despite its potential, ultrasound tomography has not been widely commercialized due to the computational complexity and limited efficiency of state-of-the-art inverse scattering techniques. The born iterative method (BIM) and its advanced variant, the distorted born iterative method (DBIM), are among the most widely used reconstruction algorithms in diffraction tomography [4]-[6]. DBIM, in particular, is known for its faster convergence compared to BIM but suffers from higher sensitivity to noise due to the iterative nature of the forward and inverse solvers. Additionally, DBIM has been successfully applied in both 2D and 3D reconstructions, as well as in layered

media and lossy environments [7]-[9]. These studies demonstrate the flexibility of DBIM, though the computational burden remains a significant challenge, as each iteration requires solving large-scale matrix equations, making real-time implementation impractical for many clinical applications [10]. DBIM, in particular, is known for its faster convergence compared to BIM but suffers from higher sensitivity to noise due to the iterative nature of the forward and inverse solvers. Additionally, the computational burden of these methods remains a significant challenge, as each iteration requires solving large-scale matrix equations, making real-time implementation impractical for many clinical applications.

Several studies have attempted to mitigate these computational and noise-related challenges. For instance, edge detection methods were incorporated into DBIM to enhance convergence speed and improve reconstruction quality [1]. However, this approach does not fully address the issue of noise sensitivity and may introduce artifacts in highly scattering environments. Another notable advancement is the use of the multi-level fast multi-pole algorithm (MLFMA) as a forward solver to accelerate the reconstruction process [11]. While MLFMA effectively reduces computation time, it incurs a high setup cost and demands extensive pre-processing, making practical implementation difficult. To stabilize DBIM in the presence of noise, Tikhonov regularization has traditionally been employed to solve the inverse problem by incorporating linear measurements of pressure signals [12]. While Tikhonov regularization mitigates some ill-posedness, it does not effectively suppress noise, often leading to degraded reconstruction quality in noisy environments. Several machine learning techniques have been explored for ultrasound tomography. For instance, Cheng *et al.* [13] proposed a deep learning method for limited-angle prostate imaging, while Shi *et al.* [14] focused on time of flight (TOF) extraction in bone ultrasound tomography. These methods highlight the potential of data-driven approaches in improving image quality. Further developments in deep learning-based tomographic reconstruction have been reported in [15], [16], where sparse sampling and general tomographic inversion were enhanced using convolutional architectures. Additional studies demonstrated fast learning-based approaches for ultrasound speed mapping [17], [18]. Despite these advances, deep learning models often require extensive training datasets and computational resources, making their real-time deployment challenging. Despite these advances, deep learning models often require extensive training datasets and computational resources, making their real-time deployment challenging. To address this, we propose an alternative k-nearest neighbors (KNN)-based machine learning denoising approach to enhance the robustness of DBIM reconstructions. Unlike deep learning methods that rely on data-driven feature extraction, KNN denoising leverages local neighborhood information to suppress noise while preserving structural details, making it particularly suitable for iterative reconstruction frameworks like DBIM. The simplicity and efficiency of KNN make it an attractive choice for real-time tomographic imaging applications, particularly in scenarios with limited training data or computational constraints. Ultrasound tomography is a significant imaging modality, particularly in breast cancer detection, soft tissue imaging, and non-destructive testing (NDT), where high-resolution and low-cost solutions are vital. The proposed KNN-filtered DBIM addresses key limitations in conventional methods by offering a low-complexity, training-free denoising strategy suitable for clinical and real-time applications. This work presents a novel integration of KNN-based denoising within the DBIM framework, which, to the best of our knowledge, has not been previously reported in ultrasound tomography. While DBIM and KNN are individually well-established, the methodological innovation lies in the adaptive KNN filtering applied in each iterative update of DBIM, effectively enhancing noise suppression without compromising structural resolution. This novel integration addresses the critical limitations of conventional regularization, particularly under high-noise scenarios, and thus represents a substantial advancement beyond existing approaches.

The remainder of this paper is organized as follows. Section 2 describes the theoretical background of the DBIM and presents the proposed integration of KNN-based denoising into the reconstruction framework. Section 3 provides simulation results to evaluate the effectiveness of the proposed method under various noise conditions. Section 4 discusses the key findings, compares them with existing approaches, highlights the implications and limitations, and outlines potential directions for future research. Finally, Section 5 concludes the paper by summarizing the main contributions and results.

2. METHOD

2.1. DBIM

The region of interest (ROI) encompasses the reconstructed object, which is centered at the origin of a two-dimensional space and discretized into an N×N grid of square pixels, each with a side length of h. The system includes N_t transmitters and N_r receivers. Figure 1 provides a schematic representation of the geometrical and acoustic setup of the ultrasound tomography system.

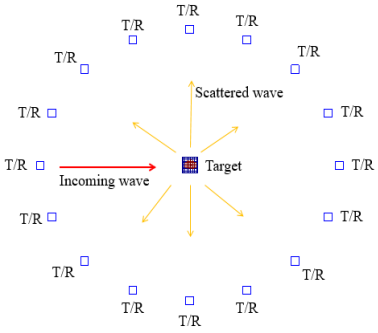

Figure 1. Ultrasound tomography imaging system

Given the circular scattering region illustrated in Figure 1, the object function can be determined using:

$$O(r) = \begin{cases} k_1(r)^2 - k_2^2 = \omega^2\left(\frac{1}{c_1^2} - \frac{1}{c_2^2}\right) \; if \; r \le R \\ 0 \; if \; r > R \end{cases} \quad (1)$$

where c_1 and c_2 represent the speed of sound within the object and in water, respectively. The ultrasound frequency is denoted by f, while ω corresponds to the angular frequency, given by $\omega = 2\pi f$. Additionally, R signifies the radius of the object.

To acquire the scattered data, we establish a measurement configuration for the transmitters and receivers. At any given moment, only a single transmitter and a single receiver are active, corresponding to one measured data point. Assuming that density variations are negligible, the inhomogeneous wave equation is expressed as:

$$\left(\nabla^2 + k_0^2(r)\right)p(r) = -O(r)p(r) \quad (2)$$

where $k_0 = \omega/c_0$ represents the wavenumber in the reference medium (i.e., water), and $p(r)$ denotes the total pressure field.

By solving (2), the scattered pressure can be expressed in an integral form using the Green's function as:

$$p^{sc}(r) = p(r) - p^{inc}(r) = \int\int O(r)p(r)G(|r - r'|) \quad (3)$$

where $p^{inc}(r)$ represents the incident pressure, and G denotes the free-space Green's function. In (3) can be solved using the method of moments, employing sinc basis functions and delta functions [19].

The pressure at the grid points can be represented as an $N^2 \times 1$ vector,

$$p = p^{inc} + C^*D(O^*)p^* \quad (4)$$

and the scattered pressure can also be determined as a scalar value.

$$p^{sc} = B_i^*D(O^*)p^* \quad (5)$$

where B_i^* is a $1 \times N^2$ vector derived from a matrix constructed using the Green's coefficient $G_0(r, r')$ for each pixel to the i^{th} receiver. The matrix $\bar{C}$ is an $N^2 \times N^2$ matrix formed by Green's coefficient among all pixels in the meshing area. The operator $D(\cdot)$ converts a vector into a diagonal matrix. Detailed computations of B_i^* and C^* can be found in [19].

If N_t transmitters and N_r receivers are employed, the scattered pressure signal can be represented as a vector of size $N_tN_r \times 1$, which is derived from (5) as:

$$p^{sc} = B_i^*D(O^*)p^* = MO^* \quad (6)$$

where $M = BD(p^*)$ is the matrix whose size is $N_t N_r \times N^2$

Since the Green's function satisfies the same differential equation as the pressure field, the forward solver is utilized to compute the Green's function for an arbitrary reference background. Given an initial value O_0^* and the corresponding reference background at time step k, the object function at step $k+1$ is updated as:

$$O_{k+1}^* = O_k^* + \Delta O_k \quad (7)$$

where ΔO is the update of the object function which can be deduced from (6) as:

$$\Delta p^{*sc} = M \Delta O \quad (8)$$

Obviously, there is an iterative process in DBIM in order to estimate the object function O^*. Moreover, in each DBIM step, we need another iterative process mentioned in the next subsection.

2.2. Inverse problem

It is well known that the matrix M is ill-conditioned, meaning that small measurement errors in the surface data can result in significant perturbations in the reconstruction outcome. The inverse solver matrix M is weakly diagonal and ill-conditioned due to the placement of detectors outside the meshing area. Consequently, it is often reformulated as a least-squares problem:

$$n||\Delta p^{*sc} - M\Delta O^*||_2 \quad (9)$$

where the symbol $||\ ||_2$ represents the Euclidean norm of vector space.

In conventional methods [20], the estimation of ΔO^* at the time step k can be performed by using Tikhonov regularization [12]:

$$\Delta O_k^* = min||\Delta p^{*sc} - M\Delta O^*||2^2 + \gamma||\ \Delta O^*||2^2 \quad (10)$$

where Δp^{*sc} represents the difference between the predicted and measured scattered fields and γ is the regularization parameter. The regularized solution is expressed as:

$$\Delta O\ = \sum_{i=1}^{r} \sigma_i u_i^T g/[(\sigma_i + \gamma)v_i] \quad (11)$$

where u_i and v_i are the component of the two matrixes U and V that satisfy:

$$M = U\Sigma VT\ = \sum_{i=1}^{r} \sigma_i u_i^T \quad (12)$$

where $\Sigma = diag(\sigma_1, \sigma_2, .. \sigma_r)$ with $\sigma_1 \geq \sigma_2 \geq \cdots \geq \sigma_r > 0$ and $U^T U = V^T V = I$. We assume that σ_r is the smallest nonzero singular value that we wish to retain.

From (11), it is evident that the regularization parameter γ must be carefully selected, as it plays a crucial role in maintaining the stability of the system [20]. A large γ value results in a rough reconstructed image, whereas a small γ increases computational complexity. These data are processed using the DBIM to reconstruct the speed of sound contrast. This approach enables the detection of tissue presence within the medium. DBIM relies on the Born approximation to iteratively solve the nonlinear inverse scattering problem. Algorithm 1 presents the calculation process of the DBIM as follows:

Algorithm 1. The distorted born iterative method

Select the positions of the transmitters and detectors as illustrated in Figure 1.

Choose initial values: $O_0^*=0$ and $p_0^*=p^{*inc}$ as shown in (15)

While n<N_{max} or RRE<ε

1. Calculate B^* and C^*
2. Calculate p^* and p^{*sc} corresponds to O_n^* using (4) and (5)
3. Calculate RRE corresponds to O_n^*
4. Calculate the ΔO_n^* by solving (10)
5. Calculate a new value of O_{n+1}^* by using (7)
6. n=n+1

End.

In Algorithm 1, the relative residual error is defined by:

$$RRE = ||\mathrm{M}\Delta O^{*} - \Delta p^{*sc} measured\ ||/||\Delta p^{*sc} measured|| \quad (13)$$

The relative residual error (RRE) is computed at each iteration. The iterative process will terminate when the RRE falls below a predefined tolerance or when the number of iterations reaches the maximum limit Nmax.

2.3. KNN for denoising in DBIM

The KNN denoising approach is a machine learning-based technique that enhances the DBIM by reducing noise in the reconstructed images. Traditional DBIM suffers from high noise sensitivity, which can degrade image quality and slow down convergence. By integrating KNN filtering into the iterative process, noise can be adaptively suppressed while preserving important structural details. KNN denoising leverages the spatial correlation among neighboring data points to smooth out noise while maintaining the integrity of the signal. This makes it particularly effective for ill-conditioned inverse problems such as DBIM-based tomographic reconstruction. DBIM is widely used in diffraction tomography due to its ability to iteratively refine reconstructions of small-scale structures. However, its high sensitivity to noise remains a major limitation, particularly in scenarios where the input data is contaminated by measurement errors or system instability. Traditional regularization is commonly used to address this issue, but it does not effectively remove noise, especially when dealing with strong scattering environments. KNN filtering is introduced as an alternative approach to improve noise robustness without significantly increasing computational complexity. The key advantages of using KNN in DBIM include: (a) preservation of structural details: Unlike traditional smoothing filters, KNN does not blur edges or distort fine features in the reconstructed images; (b) adaptability to nonlinear data: KNN operates based on similarity metrics rather than fixed transformations, making it suitable for complex biomedical imaging scenarios; and (c) computational efficiency: KNN does not require pre-training, making it a lightweight and easy-to-integrate solution within the iterative DBIM framework. KNN denoising is applied within the DBIM framework as: i) noise identification: at each iteration of DBIM, the reconstructed field is affected by noise, which can cause numerical instability and image degradation; ii) local neighborhood selection: for each pixel (or grid point) in the reconstructed image, a set of K nearest neighbors is identified based on Euclidean distance; iii) weighted averaging: the intensity value of the target pixel is replaced with the weighted mean of its K-nearest neighbors. This step smooths out noise while preserving high-contrast features; and iv) iterative refinement: the denoised image is fed back into the next DBIM iteration, enhancing stability and accelerating convergence. Mathematically, the denoised value for a pixel x_i is given by:

$$x_i' = \frac{1}{K}\sum_{j\in N(i)} x_i \quad (14)$$

where $N(i)$ represents the set of K-nearest neighbors of x_i.

The KNN filter in this study was implemented with K=5, which provided an optimal trade-off between noise suppression and structural preservation. Several values of K (3, 5, and 7) were tested experimentally; while smaller K values led to insufficient denoising, larger values tended to oversmooth object boundaries. The Euclidean distance metric was used to determine the nearest neighbors, and each neighbor's contribution was weighted inversely proportional to its distance from the target pixel. This configuration yielded the most stable convergence behavior and lowest reconstruction error across different noise levels, as demonstrated in the simulation results. KNN denoising is integrated directly after noise-contaminated field estimation and before the inverse problem is solved in each DBIM iteration. This integration ensures that DBIM receives a cleaner input at each iteration, leading to faster con-vergence and improved reconstruction accuracy. Algorithm 2 shows the K-nearest neighbors-filtered distorted born iterative method.

Algorithm 2. The KNN-filtered DBIM

1. Initialize DBIM with measured scattering data.
2. Add Gaussian noise to simulate real-world measurement uncertainties.
3. Apply KNN-based filtering on the scattered field to remove high-frequency noise components.
4. Use the denoised data to update the contrast function using the DBIM iterative process.
5. Repeat steps 3-4 until convergence criteria are met.

Unlike median, bilateral, or wavelet-based denoisers that either blur edges or require transform-domain tuning, and unlike computationally intensive methods such as BM3D or NLM, our KNN-based

approach provides a favorable trade-off: training-free, computationally lightweight, locally adaptive smoothing that preserves structural edges and is straightforward to embed into each DBIM iteration.

The overall workflow of the proposed KNN-filtered DBIM is illustrated in Figure 2. The process begins with initializing the DBIM using measured scattered field data, followed by the addition of Gaussian noise to emulate realistic measurement uncertainties. A KNN-based denoising step is then applied to the scattered field to suppress high-frequency noise components while preserving structural information. The denoised data are subsequently used in the DBIM iterative update to refine the contrast function. These filtering and updating steps are repeated until the convergence criteria are satisfied, yielding the final reconstructed sound-speed distribution.

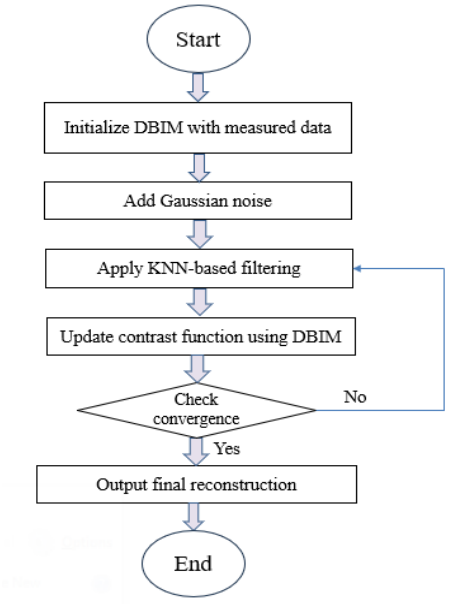

Figure 2. Flowchart of the proposed KNN-filtered DBIM

The computational cost of the proposed KNN-filtered DBIM was slightly higher than that of the standard DBIM due to the additional denoising step. On average, the KNN-based filtering increased the total computation time by approximately 8–10% per iteration, which is negligible compared with the overall DBIM reconstruction time. Unlike deep-learning-based denoisers, the KNN operation requires no model training and only involves simple distance computations, keeping the method lightweight and computationally efficient. Therefore, the proposed approach achieves a favorable balance between improved reconstruction quality and minimal added computational overhead.

3. RESULTS AND DISCUSSION

The DBIM implementation and our proposed configuration are validated using simulation on target with moderate speed contrast. Simulated data were generated for an infinitely long circular cylinder, discretized into an $N \times N = 12 \times 12$ pixel grid. The cylinder has a radius of 7.3 mm, an ultrasound signal frequency of 0.5 MHz, and a sound speed contrast of 10%. The system includes N_t=12 transmitters and N_r=12 receivers. The transmitters are positioned at 11 evenly spaced locations along a circular path surrounding the object. For each transmitter, 12 detectors are placed on the opposite side of the circle to capture the scattered signals. The incident pressure for a zero-order Bessel beam in a two-dimensional case is given by:

$$p^{*inc} = J_0(k_0|r - r_k|) \tag{15}$$

where J_0 is the 0^{th} order Bessel function and $|r - r_k|$ is the distance between the transmitter and the k^{th} point in the ROI. Figure 3 is the ideal object function corresponding to (1). In order to have a quantitative comparison, (13) can be used to calculate the RRE for each case.

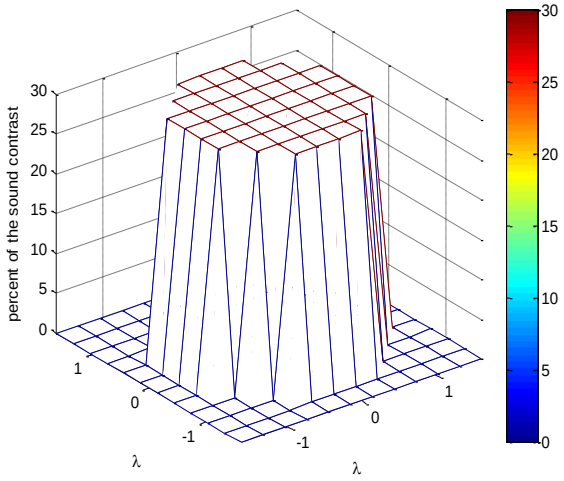

Figure 3. Ideal object function (one object in the region of interest). Color bar indicates percent of sound-speed contrast (%)

Figure 4 shows the normalized reconstruction error after the first iteration for DBIM and KNN-filtered DBIM at signal-to-noise ratio (SNR) levels of 6 dB, 3 dB, and 1 dB. The corresponding reconstructed sound-speed maps are displayed in Figure 5; visual inspection indicates improved structural preservation with KNN filtering.

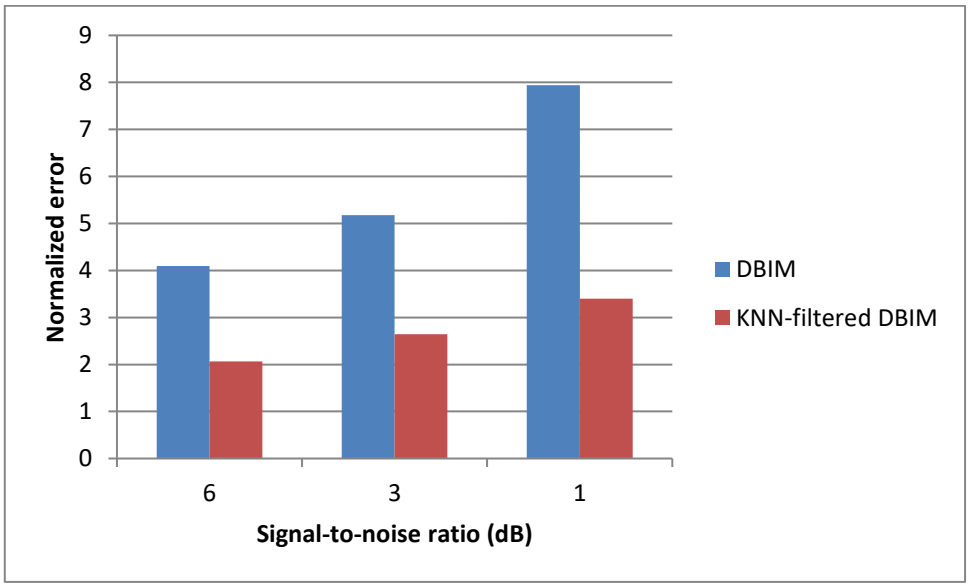

Figure 4. Normalized error of the DBIM and KNN-filtered DBIM with various signal-to-noise ratio

The results in Figure 4 indicate that the proposed KNN-based denoising method consistently reduces error across all noise levels, demonstrating superior robustness in high-noise environments. At SNR = 6 dB, as shown in Figure 6, the KNN-filtered DBIM achieves a 49.5% reduction in error compared to conventional DBIM (2.0653 vs. 4.0936). This trend continues at SNR = 3 dB as shown in Figure 7, where the proposed method reduces the error by 49% (2.6417 vs. 5.1774). The most significant improvement is observed at SNR = 1 dB, where the error is reduced by 57.2% (3.3998 vs. 7.9431), highlighting the effectiveness of KNN denoising in extremely noisy conditions. These findings suggest that integrating KNN-based denoising into DBIM enhances convergence speed by providing a cleaner initial estimate (as shown in Figure 5), reducing the burden on the iterative reconstruction process. The ability of KNN to adaptively

smooth noise while preserving structural details contributes to more stable and accurate reconstructions, particularly in low-SNR conditions. Consequently, the KNN-filtered DBIM not only accelerates the convergence rate but also improves overall image quality, making it a promising approach for tomographic imaging in challenging environments.

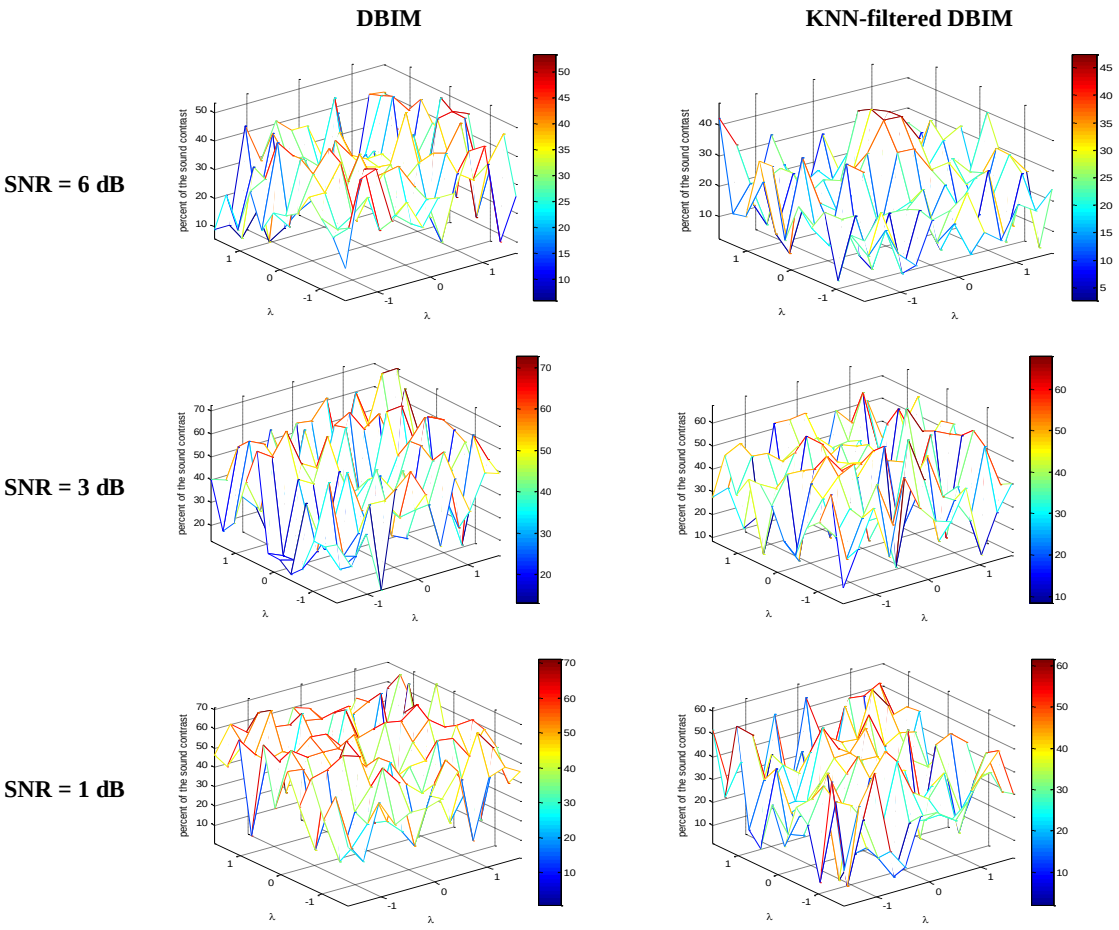

Figure 5. Reconstructed object function after the first iteration, using the conventional DBIM and proposed KNN-filtered DBIM methods in case of SNR = 6, 3, and 1 dB, respectively. Colorbar indicates percent of sound-speed contrast (%)

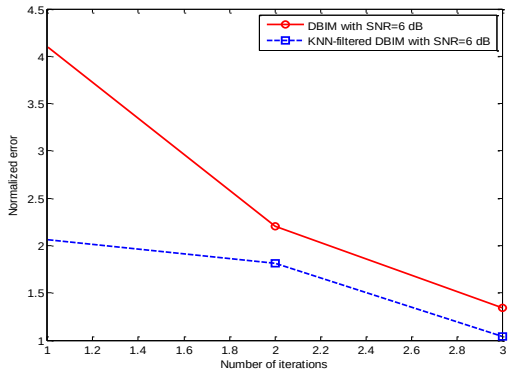

Figure 6. The normalization error after the first three iterations using the conventional DBIM and proposed KNN-filtered DBIM method in case of SNR = 6 dB

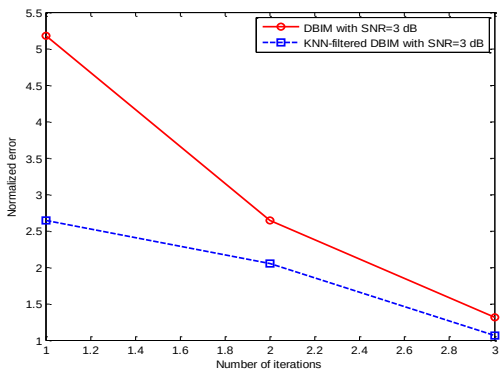

Figure 7. The normalization error after the first three iterations using the conventional DBIM and proposed KNN-filtered DBIM method in case of SNR = 3 dB

Figure 8 plots normalized error across the first three iterations at SNR = 1 dB, demonstrating faster error reduction for the KNN-filtered scheme. The result demonstrates the effectiveness of the KNN-filtered DBIM approach in reducing reconstruction errors compared to conventional DBIM under high-noise conditions. Over three iterations, the normalized error of the proposed method remains consistently lower than that of the traditional DBIM. In the first iteration, the error reduction is particularly significant, with the KNN-filtered DBIM achieving a 57.2% lower error than the conventional approach. This trend continues across subsequent iterations, showing an overall improvement in reconstruction accuracy. The results indicate that KNN-based denoising effectively removes noise before the iterative reconstruction process, leading to better initial conditions and improved stability.

We further examined a more complex scenario consisting of two circular objects located within the region of interest, as illustrated by the ideal object function in Figure 9. This configuration introduces stronger multiple-scattering interactions and overlapping diffraction patterns, posing a more challenging reconstruction problem compared with the single-object case. The reconstruction performance of the conventional DBIM and the proposed KNN-filtered DBIM was evaluated and compared under this setting at an input SNR of 1 dB. The normalized reconstruction errors for three successive iterations were 7.34, 4.09, and 2.41 for DBIM, and 4.99, 3.58, and 2.08 for the KNN-filtered DBIM, respectively. The results clearly indicate that the proposed approach achieves faster error reduction and superior reconstruction fidelity, effectively mitigating noise and preserving the structural boundaries of both inclusions.

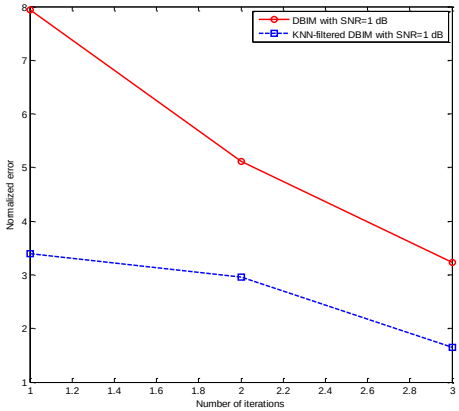

Figure 8. The normalization error after the first three iterations using the conventional DBIM and proposed KNN-filtered DBIM method in case of SNR = 1 dB

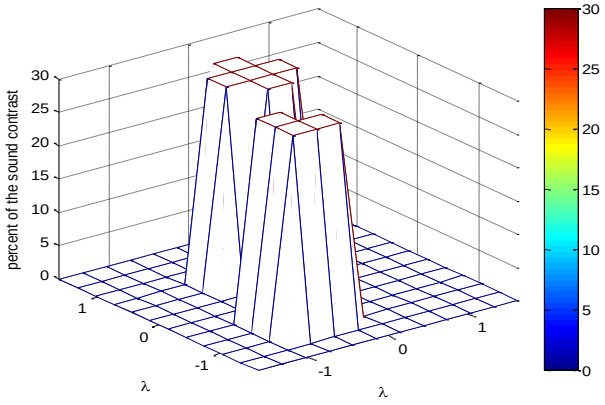

Figure 9. Ideal object function (two objects in the region of interest). Color bar indicates percent of sound-speed contrast (%)

The effectiveness of KNN denoising in DBIM depends on factors such as noise level, object complexity, and spatial resolution. It is particularly beneficial when the dataset has moderate to high levels of noise, where traditional regularization methods fail to maintain image quality; the reconstruction problem is highly ill-conditioned, requiring robust denoising techniques; fine structural details need to be preserved, such as in medical ultrasound imaging or non-destructive testing. Simulation results confirm that KNN denoising consistently improves DBIM performance by reducing reconstruction artifacts and enhancing SNR. The proposed KNN-based DBIM framework can be advantageous in various biomedical and industrial applications, including medical ultrasound tomography for high-resolution tissue imaging; breast cancer detection, where improved sound-speed maps enable better lesion characterization; non-destructive evaluation (NDE) of materials using ultrasound-based imaging. By providing better noise suppression and reconstruction accuracy, this approach can make ultrasound tomography more viable for clinical and industrial adoption. By applying KNN-based machine learning denoising in DBIM, this study introduces a efficient approach to enhance reconstruction stability, noise robustness, and convergence speed. Unlike conventional regularization techniques, KNN effectively adapts to local variations in the dataset, making it highly effective for inverse scattering problems. The experimental results demonstrate significant improvements in image quality, error reduction, and iterative efficiency, confirming that KNN-based denoising is a promising enhancement for DBIM in practical biomedical imaging applications.

To further validate the robustness of the proposed method, we extended the analysis by introducing another lightweight denoising baseline-the median filter-within the DBIM iterative framework. This comparison aims to examine whether the improvement achieved by the KNN-based denoising originates from its adaptive neighborhood weighting or merely from generic local smoothing. Figure 10 illustrates the normalized reconstruction errors across three successive iterations for conventional DBIM, median-filtered DBIM, and the proposed KNN-filtered DBIM at an input SNR of 1 dB. The quantitative results show that the proposed KNN-filtered DBIM achieves the lowest reconstruction error (3.40→1.65) compared with median-filtered DBIM (6.77→2.41) and conventional DBIM (7.94→3.23). This represents an error reduction of approximately 49% relative to DBIM and 32% relative to median filtering after the third iteration. The KNN-based approach converges faster and preserves structural boundaries more effectively, demonstrating its superior ability to suppress noise without over smoothing object edges. Unlike the median filter, which applies uniform local averaging and tends to blur fine details, the KNN filter adaptively weights neighboring pixels based on similarity, leading to enhanced edge fidelity and stability in low-SNR conditions. These findings confirm that the proposed KNN-filtered DBIM provides a more accurate and robust reconstruction framework while maintaining computational efficiency comparable to other lightweight denoisers.

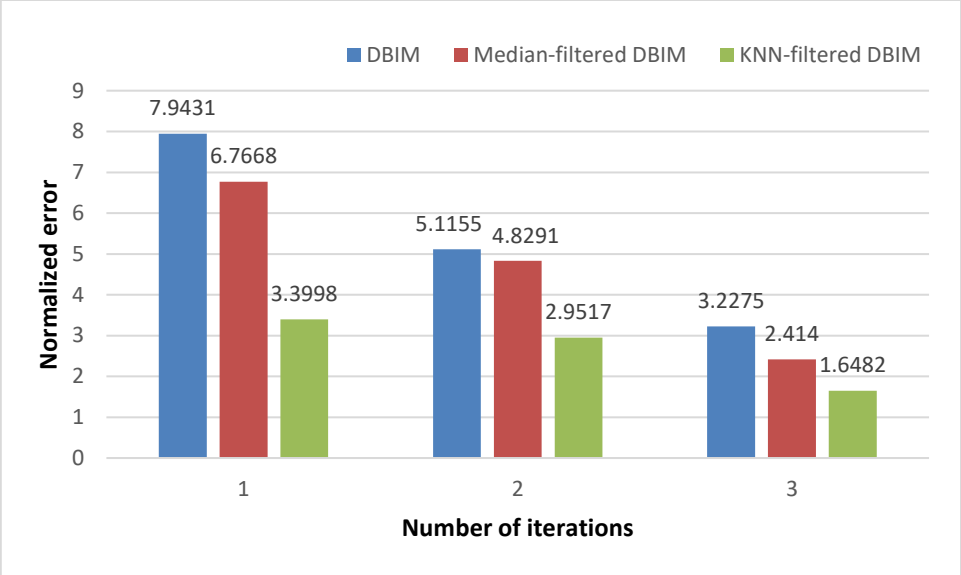

Figure 10. Normalized reconstruction error versus iteration number for the three methods-conventional DBIM, median-filtered DBIM, and KNN-filtered DBIM-at SNR = 1 dB

4. RESULT AND DISCUSSION

The central contribution of this work lies in the integration of a simple yet effective KNN-based denoising mechanism into the DBIM reconstruction framework. Unlike conventional DBIM approaches that rely solely on regularization or heavy deep-learning-based post-processing, the proposed method embeds adaptive, data-driven noise suppression directly within each iteration. This conceptual modification enhances convergence stability and reconstruction fidelity under strong noise conditions while maintaining low computational complexity. The approach demonstrates that classical, non-parametric techniques such as KNN can be successfully hybridized with iterative tomographic algorithms to achieve robust and efficient ultrasound image reconstruction. This study addresses the challenge of noise sensitivity and slow convergence in conventional DBIM reconstructions, particularly under SNR conditions. To overcome this limitation, a KNN-based denoising step was integrated into the DBIM iterative loop, forming the proposed KNN-filtered DBIM algorithm. Simulation results demonstrated that the proposed method significantly improves reconstruction fidelity and convergence speed compared with both standard DBIM and median-filtered DBIM, while maintaining computational efficiency. These findings suggest that incorporating simple, adaptive, non-parametric filters such as KNN into iterative imaging frameworks can offer a practical and lightweight alternative to complex deep-learning-based denoising approaches for robust tomographic ultrasound reconstruction.

This study has demonstrated the effectiveness of incorporating a KNN-based denoising strategy into the DBIM framework to improve the quality and robustness of ultrasound tomographic reconstruction under

noisy conditions. The simulation results clearly indicate that the proposed KNN-filtered DBIM method consistently outperforms the conventional DBIM approach in terms of normalized error and structural preservation, especially in low environments. The error reduction reached up to 57.2% at 1 dB SNR, and the visual quality of the reconstructed sound-speed maps was substantially improved after even a single iteration.

Compared to existing denoising and regularization approaches in DBIM, such as Tikhonov regularization and edge-preserving priors [1], [12], the KNN-based method offers several advantages. The proposed method is training-free, simple to implement, and computationally efficient. Moreover, while traditional regularization techniques aim to stabilize the inverse problem mathematically, they often struggle to adapt to spatially varying noise or preserve fine structural details. In contrast, KNN filtering leverages local spatial relationships and performs adaptive smoothing that maintains edge information critical for high-resolution tomographic imaging. The implications of these findings are notable. The integration of KNN filtering into DBIM provides a lightweight and flexible enhancement to an already well-established reconstruction algorithm, enabling its deployment in clinical or real-time applications where computational resources and data availability are limited. This is especially important for point-of-care ultrasound systems or low-cost imaging platforms used in remote or resource-constrained environments. Furthermore, the approach preserves the physical interpretability of the DBIM framework while improving its robustness to measurement noise, a long-standing challenge in ultrasound tomography.

The main limitations of this study have been clearly stated in the revised manuscript. The proposed KNN-filtered DBIM was evaluated only in two-dimensional simulations, and the KNN parameter K was kept fixed throughout all experiments. These constraints may limit the generalization of the results to more complex three-dimensional or heterogeneous media. Future work will address these limitations by extending the method to 3D configurations and implementing an adaptive KNN scheme where K is optimized dynamically during iterations.

Future research should focus on validating the proposed method using experimental datasets from actual ultrasound hardware. Further work may also explore the integration of adaptive KNN parameter selection, or hybrid approaches combining KNN with learning-based models to balance generalization and interpretability [21], [22]. Extending the approach to three-dimensional imaging, as well as applying it to attenuation imaging in addition to sound-speed reconstruction, could open new directions in high-fidelity ultrasound tomography. Beside that, new century is the era in which there is a large quantity of data, and that number is increasing. When dealing with such large amounts of data, the usual performance of computers is inadequate, so we need ultrasound hardware more powerful and more intelligence is required to response with the current explosion of big data [23]-27].

5. CONCLUSION

This paper has successfully introduced a KNN-based machine learning denoising approach into the DBIM to enhance reconstruction stability and reduce noise sensitivity. The conventional DBIM framework, while effective for tomographic imaging, suffers from high sensitivity to noise and slow convergence in challenging conditions. By integrating KNN filtering into the iterative reconstruction process, we have demonstrated significant improvements in both reconstruction accuracy and convergence stability. Unlike conventional regularization techniques such as Tikhonov regularization, which only alleviates ill-posedness without effectively reducing noise, the proposed KNN-based approach leverages local neighborhood relationships to perform adaptive noise suppression, leading to better noise robustness and improved image fidelity. A simulation scenario involving sound-speed contrast reconstruction has been conducted to compare the performance of the conventional DBIM method and the proposed KNN-enhanced DBIM framework. The results, analyzed through both reconstructed object functions and relative residual errors, confirm that the proposed approach outperforms traditional DBIM in terms of noise resilience, convergence speed, and overall image quality. Specifically, our findings indicate that KNN-based denoising reduces reconstruction artifacts while preserving crucial structural details, making it a promising alternative to standard noise suppression techniques in iterative tomographic imaging. For further work, we will implement an adaptive KNN where K is optimized per iteration using cross-validation on a validation set.

FUNDING INFORMATION

Authors state no funding involved.

AUTHOR CONTRIBUTIONS STATEMENT

This journal uses the Contributor Roles Taxonomy (CRediT) to recognize individual author contributions, reduce authorship disputes, and facilitate collaboration.

Name of Author	C	M	So	Va	Fo	I	R	D	O	E	Vi	Su	P	Fu
Nguyen Quang Huy	✓	✓	✓	✓	✓	✓	✓	✓	✓	✓	✓	✓	✓	✓
Nguyen Truong Thang	✓	✓			✓					✓	✓	✓		

C : **C**onceptualization
M : **M**ethodology
So : **So**ftware
Va : **Va**lidation
Fo : **Fo**rmal analysis
I : **I**nvestigation
R : **R**esources
D : **D**ata Curation
O : Writing - **O**riginal Draft
E : Writing - Review & **E**diting
Vi : **Vi**sualization
Su : **Su**pervision
P : **P**roject administration
Fu : **Fu**nding acquisition

CONFLICT OF INTEREST STATEMENT

Authors state no conflict of interest.

DATA AVAILABILITY

The data that support the findings of this study are available from the corresponding author, upon reasonable request.

REFERENCES

[1] L. T. Theu, T. Quang-Huy, T. Duc-Nghia, V. K. Solanki, T. Duc-Tan, and J. M. R. S. Tavares, "High Sound-Contrast Inverse Scattering by MR-MF-DBIM Scheme," *Electronics*, vol. 11, no. 19, p. 3203, Oct. 2022, doi: 10.3390/electronics11193203.

[2] J. Wiskin, D. T. Borup, S. A. Johnson, M. Berggren, T. Abbott, and R. Hanover, "Full-Wave, Non-Linear, Inverse Scattering," pp. 183–193, 2007, doi: 10.1007/1-4020-5721-0_20.

[3] A. Abubakar, T. M. Habashy, P. M. van den Berg, and D. Gisolf, "The diagonalized contrast source approach: an inversion method beyond the Born approximation," *Inverse Problems*, vol. 21, no. 2, pp. 685–702, 2005, doi: 10.1088/0266-5611/21/2/015.

[4] A. Saba, C. Gigli, A. B. Ayoub, and D. Psaltis, "Physics-informed neural networks for diffraction tomography," *Advanced Photonics*, vol. 4, no. 06, 2022, doi: 10.1117/1.ap.4.6.066001.

[5] W. C. Chew and Y. M. Wang, "Reconstruction of two-dimensional permittivity distribution using the distorted Born iterative method," *IEEE Transactions on Medical Imaging*, vol. 9, no. 2, pp. 218–225, 1990, doi: 10.1109/42.56334.

[6] R. J. Lavarello and M. L. Oelze, "Tomographic Reconstruction of Three-Dimensional Volumes Using the Distorted Born Iterative Method," *IEEE Transactions on Medical Imaging*, vol. 28, no. 10, pp. 1643–1653, 2009, doi: 10.1109/tmi.2009.2026274.

[7] F. Li, Q. H. Liu, and L.-P. Song, "Three-Dimensional Reconstruction of Objects Buried in Layered Media Using Born and Distorted Born Iterative Methods," *IEEE Geoscience and Remote Sensing Letters*, vol. 1, no. 2, pp. 107–111, 2004, doi: 10.1109/lgrs.2004.826562.

[8] L. T. Theu, Q.-H. Tran, V. K. Solanki, T. R. Shemeleva, and D.-T. Tran, "Influence of the multi-resolution technique on tomographic reconstruction in ultrasound tomography," *International Journal of Parallel, Emergent and Distributed Systems*, vol. 36, no. 6, pp. 579–593, 2021, doi: 10.1080/17445760.2021.1967350.

[9] C. Lu, J. Lin, W. Chew, and G. Otto, "Image Reconstruction with Acoustic Measurement Using Distorted Born Iteration Method," *Ultrasonic Imaging*, vol. 18, no. 2, pp. 140–156, 1996, doi: 10.1177/016173469601800204.

[10] A. Javaherian and B. Cox, "Ray-based inversion accounting for scattering for biomedical ultrasound tomography," *Inverse Problems*, vol. 37, no. 11, p. 115003, 2021, doi: 10.1088/1361-6420/ac28ed.

[11] A. J. Hesford and W. C. Chew, "Fast inverse scattering solutions using the distorted Born iterative method and the multilevel fast multipole algorithm," *The Journal of the Acoustical Society of America*, vol. 128, no. 2, pp. 679–690, 2010, doi: 10.1121/1.3458856.

[12] G. H. Golub, P. C. Hansen, and D. P. O'Leary, "Tikhonov Regularization and Total Least Squares," *SIAM Journal on Matrix Analysis and Applications*, vol. 21, no. 1, pp. 185–194, 1999, doi: 10.1137/s0895479897326432.

[13] A. Cheng *et al.*, "Deep learning image reconstruction method for limited-angle ultrasound tomography in prostate cancer," *Medical Imaging 2019: Ultrasonic Imaging and Tomography*. SPIE, 2019, doi: 10.1117/12.2512533.

[14] Q. Shi, T. Zhou, Y. Li, C. Liu, and D. Ta, "Deep Learning for TOF Extraction in Bone Ultrasound Tomography," *IEEE Transactions on Computational Imaging*, vol. 8, pp. 1063–1073, 2022, doi: 10.1109/tci.2022.3225670.

[15] G. Wang, J. C. Ye, and B. De Man, "Deep learning for tomographic image reconstruction," *Nature Machine Intelligence*, vol. 2, no. 12, pp. 737–748, 2020, doi: 10.1038/s42256-020-00273-z.

[16] X. Long, J. Chen, W. Liu, and C. Tian, "Deep Learning Ultrasound Computed Tomography Under Sparse Sampling," *IEEE Transactions on Ultrasonics, Ferroelectrics, and Frequency Control*, vol. 70, no. 9, pp. 1084–1100, 2023, doi: 10.1109/tuffc.2023.3299954.

[17] S. Prasad and M. Almekkawy, "A fast and efficient ultrasound tomography using deep learning," *The Journal of the Acoustical Society of America*, vol. 148, no. 4_Supplement, p. 2450, 2020, doi: 10.1121/1.5146762.

[18] X. Qu, G. Yan, D. Zheng, S. Fan, Q. Rao, and J. Jiang, "A Deep Learning-Based Automatic First-Arrival Picking Method for Ultrasound Sound-Speed Tomography," *IEEE Transactions on Ultrasonics, Ferroelectrics, and Frequency Control*, vol. 68, no. 8, pp. 2675–2686, 2021, doi: 10.1109/tuffc.2021.3074983.

[19] Y. Gao, W. Guo, and Y. Sun, "Neural Inverse Scattering With Score-Based Regularization," *2025 IEEE Conference on Computational Imaging Using Synthetic Apertures (CISA)*. IEEE, pp. 1–5, 2025, doi: 10.1109/cisa64343.2025.11091557.

[20] R. Lavarello and M. Oelze, "A study on the reconstruction of moderate contrast targets using the distorted born iterative method," *IEEE Transactions on Ultrasonics, Ferroelectrics and Frequency Control*, vol. 55, no. 1, pp. 112–124, 2008, doi: 10.1109/tuffc.2008.621.
[21] S. Subha and U. Kumaran, "Efficient Liver Segmentation using Advanced 3D-DCNN Algorithm on CT Images," *Engineering, Technology & Applied Science Research*, vol. 15, no. 1, pp. 19324–19330, 2025, doi: 10.48084/etasr.9157.
[22] A. Al-Shahrani, W. Al-Amoudi, R. Bazaraah, A. Al-Sharief, and H. Farouquee, "An Image Processing-based and Deep Learning Model to Classify Brain Cancer," *Engineering, Technology & Applied Science Research*, vol. 14, no. 4, pp. 15433–15438, 2024, doi: 10.48084/etasr.7803.
[23] A. B. A. Hassanat, "Furthest-Pair-Based Binary Search Tree for Speeding Big Data Classification Using K-Nearest Neighbors," *Big Data*, vol. 6, no. 3, pp. 225–235, 2018, doi: 10.1089/big.2018.0064.
[24] A. Almomany, W. R. Ayyad, and A. Jarrah, "Optimized implementation of an improved KNN classification algorithm using Intel FPGA platform: Covid-19 case study," *Journal of King Saud University - Computer and Information Sciences*, vol. 34, no. 6, pp. 3815–3827, 2022, doi: 10.1016/j.jksuci.2022.04.006.
[25] N. Seman and N. A. Razmi, "Machine learning-based technique for big data sentiments extraction," *IAES International Journal of Artificial Intelligence*, vol. 9, no. 3, pp. 473–479, 2020, doi: 10.11591/ijai.v9.i3.pp473-479.
[26] H. K. Omar and A. K. Jumaa, "Distributed big data analysis using spark parallel data processing," *Bulletin of Electrical Engineering and Informatics*, vol. 11, no. 3, pp. 1505–1515, 2022, doi: 10.11591/eei.v11i3.3187.
[27] A. H. Ali, M. A. Mohammed, R. A. Hasan, M. N. Abbod, M. S. Ahmed, and T. Sutikno, "Big data classification based on improved parallel k-nearest neighbor," *TELKOMNIKA (Telecommunication Computing Electronics and Control)*, vol. 21, no. 1, p. 235, 2023, doi: 10.12928/telkomnika.v21i1.24290.

BIOGRAPHIES OF AUTHORS

Nguyen Quang Huy received the Bachelor of Science with Upper Second Class Honours in Computer Science and Information Systems at Oxford Brookes University in 2014 and Master degree on Information and Communication Technology at University of Science and Technology of Hanoi and National Polytechnic Institute of Toulouse (France) in 2017. Now, he is researcher and he is working at the Institute of Information Technology, Vietnam Academy of Science and Technology. His researches focus on artificial intelligence, data mining, soft computing, and fuzzy computing. He can be contacted at email: quanghuy7889@gmail.com.

Nguyen Truong Thang received a Ph.D. in 2005 at the Japan Advanced Institute of Science and Technology (JAIST), Japan. Currently, he is a Director of the Institute of Information Technology, Vietnam Academy of Science and Technology. His major research fields include Software quality assurance, software verification, program analysis, data mining and machine Learning. He can be contacted at email: ntthang@ioit.ac.vn.